RSC Advances

PAPER

View Article Online
View Journal | View Issue

Cite this: *RSC Adv.*, 2018, **8**, 6887

A designable aminophenylboronic acid functionalized magnetic Fe_3O_4/ZIF-8/APBA for specific recognition of glycoproteins and glycopeptides†

Shanshan Li, Dongyan Li,* Long Sun, Yuewei Yao and Cheng Yao*

Received 2nd November 2017
Accepted 9th January 2018

DOI: 10.1039/c7ra12054k

rsc.li/rsc-advances

We fabricated a novel aminophenylboronic acid functionalized magnetic Fe_3O_4/zeolitic imidazolate framework-8/APBA (denoted as Fe_3O_4/ZIF-8/APBA). First, Fe_3O_4 was coated by zeolitic imidazolate framework-8 (denoted as Fe_3O_4/ZIF-8) using the hydrothermal method. Next, the phenylboronic acid functionalized triethoxysilane reagent was synthesized by 3-aminophenylboronic acid and 3-isocyanatopropyltriethoxysilane, which was modified on the surface of the Fe_3O_4/ZIF-8 nanocomposite through the sol–gel technique and electrostatic interaction as well as π–π stacking interaction. The synthetic Fe_3O_4/ZIF-8/APBA exhibited high adsorption capacity and good specificity toward glycoproteins. Moreover, the Fe_3O_4/ZIF-8/APBA possessed high saturation magnetization (51.41 emu g^{-1}) and achieved better separation in the presence of an external magnetic field. Above all, the as-designed Fe_3O_4/ZIF-8/APBA was successfully used to capture glycoproteins and identify the horseradish peroxidase (HRP) tryptic digest. This study provides a facile strategy to embellish the aminophenylboronic acid onto the nanocomposite substrate and develop a new material for the specific recognition and enrichment of glycoproteins and low-abundance glycopeptides in proteomics research.

Introduction

Protein glycosylations, one of the most common and important post-translation modifications, play crucial roles in a variety of biological activities.[1,2] Aberrant glycosylations are normally associated with disease progression, such as tumor immunology, cell division and cancer development.[3–5] Characterization and identification of glycopeptides, particularly glycosylation site occupancy and glycan heterogeneity at each glycosite, have great significance in glycoproteomics.[6–8] However, low abundant glycoproteins and glycopeptides were usually covered by high abundance non-glycoproteins and non-glycopeptides, which caused severe interference in the field of identification.[9–11] Therefore, the design of novel nanomaterials for separation and enrichment of glycoproteins and glycopeptides is necessary and plays an important role in the development of glycoproteomics.

Boronic ligands and *cis*-diol moieties of glycoproteins and glycopeptides were combined by covalent interactions in mildly basic aqueous media, while the formed boronate cyclic esters can be hydrolyzed under acidic conditions.[12] Hence, the glycoproteins and glycopeptides can be captured or released by switching the pH value.[13] Therefore, boronic acid ligand-functionalized materials have been developed in the fields of specific recognition, immobilization and enrichment of glycoproteins and glycopeptides.[14–16]

As star materials, iron oxide (Fe_3O_4) nanoparticles have received considerable attention owing to their low cost, high surface to volume ratio, remarkable magnetic response, and biological compatibility.[17,18] Based on this concept, numerous magnetic nanostructures have been used in the enrichment of glycoproteins and glycopeptides.[19–23] For example, Zhang *et al.* prepared aminophenylboronic acid functionalized magnetic nanoparticles *via* Cu(I)-catalyzed azide–alkyne cycloaddition click chemistry.[24] Ma *et al.* synthesized boronic acid functionalized magnetic carbon nanotubes through Fe^{3+} loading on the acid-treated CNTs and the modification with 1-pyrenebutanoic acid *N*-hydroxysuccinimidyl ester to bind aminophenylboronic acid *via* an amide reaction.[25] Although the above studies have achieved some success, facile and effective approaches for the separation of glycoproteins and the enrichment of glycopeptides are highly desirable. In other words, the separation of highly abundant proteins and the enrichment of low grade proteins are still great challenges.

Metal–organic frameworks (MOFs), an intriguing class of hybrid materials, exist as infinite crystalline lattices with metal

School of Chemistry and Molecular Engineering, Nanjing Tech University, Nanjing 211816, China. E-mail: lidongyan111@njtech.edu.cn; yaocheng@njtech.edu.cn

† Electronic supplementary information (ESI) available. See DOI: 10.1039/c7ra12054k

clusters and organic linkers.[26,27] Gu *et al.* introduced MOFs to achieve efficient enrichment of peptides and proteins and demonstrated the proof-of-concept by utilizing three types of MOFs.[28] Zhang *et al.* synthesized amino-functionalized metal frameworks for the enrichment of glycopeptides by hydrophilic interactions.[29] On the basis of these studies, a designable strategy for the development of a nanocomposite material based on magnetic Fe_3O_4 and a metal–organic framework was proposed and applied for the specific recognition of glycoproteins and glycopeptides through boric acid affinity.

In this study, a new type of Fe_3O_4/ZIF-8/APBA material was constructed by the hydrothermal process and sol–gel technique. In brief, 3-aminophenylboronic acid and 3-isocyanatopropyltriethoxysilane were integrated to obtain the phenylboronic acid functionalized triethoxysilane reagent, which played the role of a recognition site and was fabricated on the surface of nanocomposite substrates. ZIF-8 as a member of a subfamily of MOFs shows high porosity, good mechanical stability, and outer-surface properties.[30] These special properties make it a valuable candidate in separation and enrichment. Considering the poor separation ability from a solid–liquid system, the assembly of ZIF-8 and magnetic Fe_3O_4 nanoparticles is a good choice. Magnetic Fe_3O_4 nanoparticles exhibit a unique magnetic response, large surface area and low cytotoxicity.[31] In this study, ZIF-8 was assembled onto Fe_3O_4 nanoparticles to fabricate the core–shell Fe_3O_4/ZIF-8 nanocomposite by the hydrothermal process, which displays common and synergistic effects to develop new materials and adsorb target molecules with high capacity and magnetic manipulability. Combining the merits of the magnetic property of the Fe_3O_4 nanoparticles and the high surface to volume area of ZIF-8 as well as the interactions of boronic acid ligands with glycoproteins and glycopeptides, the hybrid Fe_3O_4/ZIF-8/APBA material exhibited magnetic manipulability, high adsorption capacity, good recyclability and specificity toward glycoproteins. Furthermore, the Fe_3O_4/ZIF-8/APBA NPs were successfully used in the enrichment of target glycopeptides from the horseradish peroxidase (HRP) tryptic digest.

Experimental

Materials

Ovalbumin (OVA), transferrin (Trf), horseradish peroxidase (HRP), lysozyme (Lyz) and bovine serum albumin (BSA) were obtained from the Beijing Solarbio Science and Technology Company. Ammonium bicarbonate (ABC), urea (urea), dithiothreitol (DTT), iodoacetamide (IAA), and trifluoroacetic acid (TFA) were purchased from J&K Scientific Ltd. 2-Methylimidazolate, 3-aminophenylboronic acid, and 3-isocyanatopropyltriethoxysilane were purchased from Aladdin. Iron(III) chloride hexahydrate ($FeCl_3 \cdot 6H_2O$, 99%), anhydrous sodium acetate (NaAc), ethylene glycol, zinc nitrate hexahydrate ($Zn(NO_3)_2 \cdot 6H_2O$, 99%), tetrahydrofuran, poly(sodium-*p*-styrenesulfonate) (PSS, 20 wt%), acetonitrile and ethanol were all purchased from Sinopharm Chemical Reagent Co., Ltd. Deionized water used for the experiments was ultrapure. All the reagents were analytically pure.

Characterization

Transmission electron microscopy (TEM) imaging was performed on a Tecnai G2 T2 S-TWIN transmission electron microscope. The identification of the crystalline phase of Fe_3O_4/ZIF-8/APBA was performed on a Rigaku D/max/2500v/pc (Japan) X-ray diffractometer, equipped with a Cu Kα source. The 2θ angles probed were from 5° to 85° at a rate of 10° min^{-1}. The infrared spectra were recorded on a Nicolet AVATAR-360 Fourier transform infrared (FTIR) spectrometer. The magnetic properties were analyzed with a vibrating sample magnetometer (VSM) (LDJ 9600-1, USA). The adsorption–desorption isotherms of nitrogen at 77 K were determined using a Micromeritics ASAP 2020 instrument. Matrix-assisted laser desorption/ionization-time-of-flight mass spectrometry (MALDI-TOF-MS) analysis was carried out on an AutoflexIII LRF200-CID TOF mass spectrometer (Bruker Daltonics, Germany). UV-vis spectrum was recorded using a TU-1900 from Beijing Purkinje General Instrument Company Limited. A matrix solution of 2,5-dihydroxybenzoic acid (DHB; 25 mg mL^{-1}) was prepared in CH_3CN/H_2O/H_3PO_4 (60 : 40 : 1, v/v/v). Equivalent amounts of the sample and DHB were sequentially dropped onto the MALDI plate for MS analysis. All MS spectra were obtained in the positive-ion reflector mode.

Synthesis of Fe_3O_4 NPs

Fe_3O_4 NPs were synthesized according to a modified hydrothermal method.[32] Briefly, $FeCl_3 \cdot 6H_2O$ (1.35 g) and NaAc (3.6 g) were dissolved in ethylene glycol (35 mL) in a poly(tetrafluoroethylene) (Teflon)-lined autoclave. After reaction at 200 °C for 12 h, the as-obtained Fe_3O_4 were collected by magnetic separation and rinsed with ultrapure water and ethanol and then dried at 50 °C overnight.

Preparation of Fe_3O_4/ZIF-8 NPs

The core–shell Fe_3O_4/ZIF-8 NPs were prepared according to a previous reference with some modification.[33] Typically, 0.05 g Fe_3O_4 was dispersed in a mixture of 0.45 mL PSS and 29.55 mL H_2O under ultrasonication for 20 min and then, it was separated using a magnetic field and washed with distilled water three times. The above product was dispersed in methanol solution under ultrasonication for 15 min to acquire a homogeneous solution and then, 0.297 g of $Zn(NO_3)_2 \cdot 6H_2O$ and 0.492 g of 2-methylimidazolate were added to the above homogeneous solution under mechanical stirring. The reaction was continued for 3 h at 50 °C for the growth of the ZIF-8 shell. The resultant Fe_3O_4/ZIF-8 nanoparticles were separated by magnetic separation and washed with ethanol three times and then dried at 50 °C overnight.

Synthesis of Fe_3O_4/ZIF-8/APBA NPs

The aminophenylboronic acid functionalized magnetic Fe_3O_4/ZIF-8 (Fe_3O_4/ZIF-8/APBA) was prepared by the sol–gel method. First, 160 mg of 3-aminophenylboronic acid monohydrate was dissolved into THF solution. Then, 3-isocyanatopropyltriethoxysilane (240 μL) was added to the above solution, which was stirred for

24 h at room temperature. The obtained phenylboronic acid functionalized triethoxysilane reagent (APBA) was added in the acetate buffer solution (0.1 mol L^{-1}, pH 5.2, 40 mL) and 40 mg of Fe_3O_4/ZIF-8 nanoparticles were dispersed homogeneously in the above solution. The reaction was allowed to proceed at room temperature for 12 h. The final Fe_3O_4/ZIF-8/APBA NPs were obtained by magnetic separation and dried at 50 °C overnight.

Protein adsorption

The adsorption experiment was performed to evaluate the binding capacity of the Fe_3O_4/ZIF-8/APBA NPs toward glycoproteins and non-glycoproteins. Three milligrams of Fe_3O_4/ZIF-8/APBA were added to the protein solution with different concentrations (0.1 mg mL^{-1} to 2.0 mg mL^{-1}) in 20 mmol L^{-1} PBS buffer solution (pH = 9.0). The supernatant and Fe_3O_4/ZIF-8/APBA were separated by external magnetic field and detected using a UV-vis spectrophotometer. The adsorption capacity (Q) of the protein was calculated using the equation below:

$$Q = (C_0 - C_t)V/W \text{ (mg g}^{-1}\text{)}$$

where C_0 (mg mL^{-1}) and C_t (mg mL^{-1}) are the initial and equilibrium concentrations of proteins, respectively; V (mL) represents the volume of protein solution; W (g) is the weight of the Fe_3O_4/ZIF-8/APBA NPs.

Enrichment of glycopeptides from the tryptic digest of HRP

Initially, 100 μL of 8 M urea (in 50 mM ABC) was added to the 1.0 mg mL^{-1} HRP solution, which was kept at 55 °C for 1 h. Then, 50 μL of 1 M DTT (in 50 mM ABC) was injected in the above solution at 55 °C and kept for another hour. Then, 100 μL of 1 M IAA (in 50 mM ABC) was added at 37 °C for 0.5 h in the dark. Finally, the HRP solution was incubated with trypsin at an enzyme/substrate ratio of 1 : 50 (w/w) at 37 °C for 16 h. The digests were diluted to 0.5 mg mL^{-1} and stored at −20 °C before further use. Fe_3O_4/ZIF-8/APBA (3 mg) was incubated in HRP digest (500 μL, 10 ng μL^{-1}) with shaking in the orbital shaker overnight. After washing with ABC (50 mM, pH 8.0), the supernatant was decanted with the help of a magnet. Then, 500 μL of TFA/CH_3CN/H_2O (1 : 50 : 49 (v/v/v)) was added to release the glycopeptides for 2 h at 25 °C, and the elution was deposited on a MALDI plate for mass spectrometric analysis.

Results and discussion

Preparation and characterization of the Fe_3O_4/ZIF-8/APBA NPs

The preparation of Fe_3O_4/ZIF-8/APBA NPs with a core–shell structure is illustrated in Scheme 1. In this protocol, Fe_3O_4 NPs were synthesized using the modified solvothermal method and then, ZIF-8 was assembled onto the surface of Fe_3O_4 NPs. ZIF-8 has high porosity, good mechanical stability, and provides the ideal conditions for further modifications, but it suffers from poor separation ability from the solid–liquid system. It is worth mentioning that magnetic Fe_3O_4 NPs have magnetic susceptibility, good biocompatibility, and low toxicity. Therefore, magnetic Fe_3O_4 NPs were embedded by ZIF-8 to obtain the

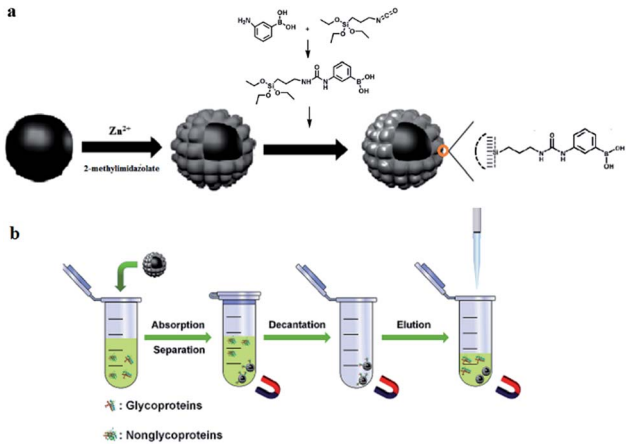

Scheme 1 The synthesis route of magnetic Fe_3O_4/ZIF-8/APBA NPs (a) and specific enrichment of glycoproteins and glycopeptides with the help of an applied magnetic field (b).

Fe_3O_4/ZIF-8 nanocomposite substrates, which combined the advantages of Fe_3O_4 and ZIF-8. Then, the Fe_3O_4/ZIF-8 NPs were functionalized by APBA through the sol–gel technique and electrostatic interaction and π–π stacking interaction due to the benzene rings. The boronic acid ligand was used to specifically recognize glycoproteins and glycopeptides.

The size and morphology of the resultant Fe_3O_4/ZIF-8/APBA NPs were investigated by TEM. As shown in Fig. 1, the average diameters of Fe_3O_4 NPs were about 360 nm (Fig. 1a). After being coated with ZIF-8, the size of the Fe_3O_4/ZIF-8 NPs increased to around 400 nm; the inset image in Fig. 1b shows that Fe_3O_4 NPs are wrapped in approximately 20 nm porous structures ZIF-8 layer. After APBA was modified, it could be observed from Fig. 1c that the thin layer was about 10 nm in the outermost layer, which illustrated that the phenylboronic acid functionalized triethoxysilane reagent (APBA) was successfully formed on the surface of Fe_3O_4/ZIF-8. The thin layer provided better site accessibility and lower mass transfer resistance for specific recognition of the glycoproteins and glycopeptides.

Vibrating sample magnetometry (VSM) at room temperature was employed to study the magnetic properties of Fe_3O_4, Fe_3O_4/ZIF-8 and Fe_3O_4/ZIF-8/APBA NPs (Fig. 2). It is clear that Fe_3O_4 and Fe_3O_4/ZIF-8 NPs have magnetic saturation (MS) values of about 60.44 and 56.24 emu g^{-1}, respectively, which are smaller than that of the corresponding bulk Fe_3O_4 (92 emu g^{-1}). In general, these values are ascribed to the addition of a dead

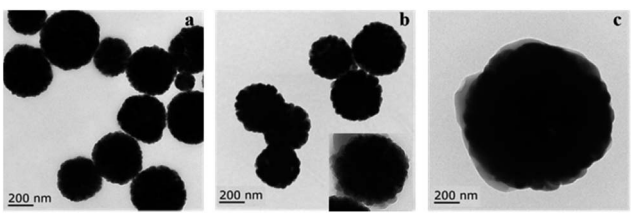

Fig. 1 TEM images of Fe_3O_4 (a), Fe_3O_4/ZIF-8 (b) and Fe_3O_4/ZIF-8/APBA NPs (c).

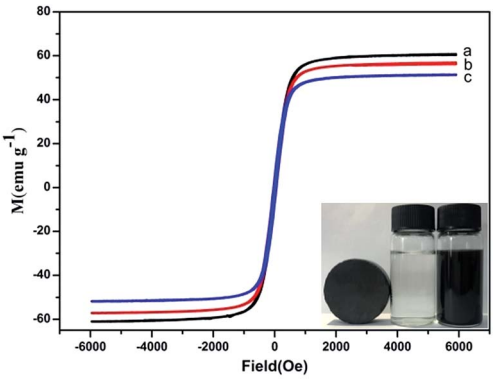

Fig. 2 Hysteresis loops of Fe_3O_4 (a), Fe_3O_4/ZIF-8 (b) and Fe_3O_4/ZIF-8/APBA NPs (c).

magnetic layer (ZIF-8) on the surface of Fe_3O_4 nanoparticles.[34,35] After APBA was functionalized on the surface of Fe_3O_4/ZIF-8, the magnetic saturation values of Fe_3O_4/ZIF-8/APBA (Fig. 2c) were about 51.41 emu g^{-1}. There was further decline on the basis of the above Fe_3O_4/ZIF-8, which illustrates that the APBA layer increased the weight fraction of the non-magnetic composite. The magnetic hysteresis loops for Fe_3O_4, Fe_3O_4/ZIF-8, and Fe_3O_4/ZIF-8/APBA exhibited an S-like shape with no coercivity and remanence. The superparamagnetic nature was beneficial for the separation process under the action of the magnetic field.[36] The Fe_3O_4/ZIF-8/APBA NPs were dispersed homogeneously in a protein solution; after the binding of target glycoproteins, the Fe_3O_4/ZIF-8/APBA NPs were quickly and easily (within 20 seconds) attracted to the wall of the glass bottle with the help of a magnet (inset of Fig. 2). This result indicated that the novel material was successfully synthesized and its magnetic saturation could be used in the separation of glycoproteins.

The X-ray powder diffraction (XRD) patterns for the synthesized Fe_3O_4, Fe_3O_4/ZIF-8, and Fe_3O_4/ZIF-8/APBA NPs are shown in Fig. 3. Six types of particle peak positions (2θ = 30.1, 35.5, 43.1, 53.4, 57.0 and 62.6) at the corresponding 2θ values are indexed as (220), (311), (400), (422), (511), and (440),

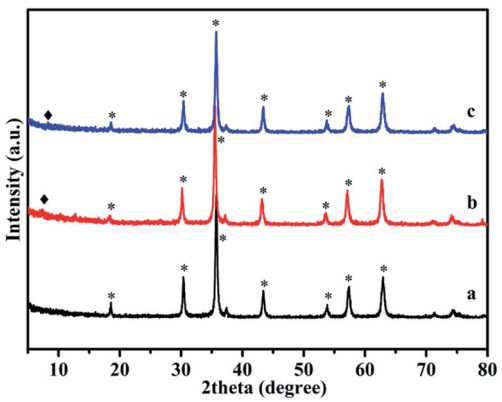

Fig. 3 XRD spectra of Fe_3O_4 (a), Fe_3O_4/ZIF-8 (b) and Fe_3O_4/ZIF-8/APBA NPs (c).

respectively, which matched well with those from the JCPDS card (no. 19-0629). A very weak diffraction peak at 2θ = 7.3° corresponding to the (011) plane of ZIF-8 is visible, which indicated that the ZIF-8 layer was relatively thin. The sharp peaks confirmed that the Fe_3O_4/ZIF-8 was crystallized and the nanocrystalline structure remains unchanged before and after modification of APBA.

FT-IR spectra of the Fe_3O_4, Fe_3O_4/ZIF-8, and Fe_3O_4/ZIF-8/APBA NPs are shown in Fig. S1.† The characteristic peak at 593 cm^{-1} was attributed to the Fe–O stretching. The peaks at 1604 and 1402 cm^{-1} are associated with carboxylate groups available from the stabilizer (Fig. S1a†). In contrast to the infrared data of Fe_3O_4, the FT-IR spectrum of Fe_3O_4/ZIF-8 displays additional adsorption bands (Fig. S1b†): the band at 449 cm^{-1} is attributed to the Zn–N stretch mode, while the bands in the spectral region of 500–1350 cm^{-1} and 1350–1500 cm^{-1} are assigned as the plane bending and stretching of imidazole ring, respectively. The C=N stretching mode is located at 1638 cm^{-1} and the peaks at 2910 cm^{-1} and 2972 cm^{-1} are attributed to the C–H stretching. In the curve of Fe_3O_4/ZIF-8/APBA, the peaks at 1398 cm^{-1}, 1459 cm^{-1}, 1624 cm^{-1} are ascribed to the B–O group (Fig. S1c†), which indicated the successful fabrication of Fe_3O_4/ZIF-8/APBA.

To further confirm the successful synthesis of Fe_3O_4/ZIF-8/APBA, XPS spectroscopy analysis was employed. As shown in Fig. 4, the XPS survey showed the characteristic peaks of N 1s (408.98 eV), Fe 2p (737.98 eV) and Zn LM2 (496.58 eV), which indicated that the imidazole group and Zn ions were present. The signal of B 1s (189.2 eV) indicated that APBA was successfully modified and Fe_3O_4/ZIF-8/APBA was fabricated. The N_2 adsorption–desorption isotherms were obtained to investigate the surface properties of Fe_3O_4/ZIF-8 and Fe_3O_4/ZIF-8/APBA (Fig. S2†). The isotherms also exhibit some nitrogen uptake as a type of hysteresis at $0.6 < P/P_0 < 1.0$, which could be due to the presence of mesopores/macropores formed by the stacking of

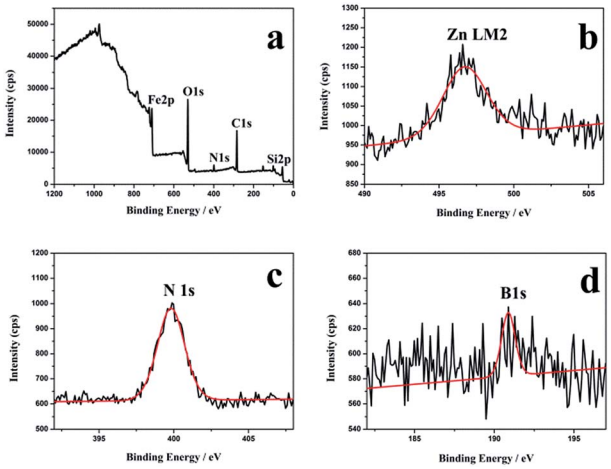

Fig. 4 XPS spectra of the as-prepared Fe_3O_4/ZIF-8/APBA. (a) XPS survey spectrum; (b) binding energy spectrum of Zn LM2; (c) binding energy spectrum of B 1s; (d) binding energy spectrum of N 1s.

microspheres. The Brunauer–Emmett–Teller surface area of the Fe_3O_4/ZIF-8 was calculated to be 70.1 m^2 g^{-1}. This result indicates the formation of ZIF-8 on the surface of Fe_3O_4. After the modification of the aminophenylboronic ligand layer, the Brunauer–Emmett–Teller surface area of Fe_3O_4/ZIF-8/APBA significantly decreased, which illustrated that the aminophenylboronic ligand layer was formed outside Fe_3O_4/ZIF-8.

Protein adsorption with Fe_3O_4/ZIF-8/APBA

In order to investigate the specific recognition of Fe_3O_4/ZIF-8/APBA toward glycoproteins OVA and Trf, the non-glycoproteins Lyz and BSA were chosen as the contrast proteins, respectively. Fig. 5 shows the adsorption capacity of four proteins. Fe_3O_4/ZIF-8/APBA NPs display significant specific adsorption towards OVA and Trf compared to Lyz and BSA. The maximum concentration of adsorption capacity of OVA and Trf was 833.33 mg g^{-1} and 603.33 mg g^{-1}, respectively. For non-glycoproteins, Lyz and BSA showed much less adsorbing capacity, suggesting that physical binding was the primary factor between the Fe_3O_4/ZIF-8/APBA NPs and the non-glycoproteins. These results illustrated that Fe_3O_4/ZIF-8/APBA had a higher adsorption capacity toward glycoproteins due to the covalent coordination between the boronic ligand and the *cis*-diols moiety of glycoproteins.

The recyclability of Fe_3O_4/ZIF-8/APBA

Desorption and regeneration is a significant indicator for the applied materials. The adsorbed glycoproteins could be eluted by adjusting the pH value of the solution because the boronate ester bond can be hydrolyzed under acidic conditions (acetate buffer (pH 4.0)). Ovalbumin (0.6 mg mL^{-1}, pH = 9.0) was adsorbed and separated by Fe_3O_4/ZIF-8/APBA five times (Fig. 6). After five cycles, the adsorption capacity of Fe_3O_4/ZIF-8/APBA NPs toward OVA did not significantly reduce, which shows the advantages of the novel material in practical applications.

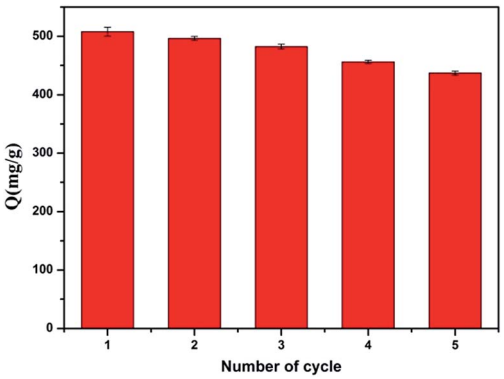

Fig. 6 Recyclability of Fe_3O_4/ZIF-8/APBA for the adsorption–desorption ability to OVA.

Glycopeptides enrichment from HRP trypic digests

The synthetic Fe_3O_4/ZIF-8/APBA NPs were utilized to evaluate the enrichment capacity for glycopeptides from the horseradish peroxidase (HRP) tryptic digests. The Fe_3O_4/ZIF-8/APBA NPs were incubated with the HRP tryptic digest and then separated by the magnetic field. The captured peptides were specifically eluted and analyzed by matrix-assisted laser desorption/ionization-time-of-flight (MALDI-TOF) mass spectrometry. Fig. 7a shows the MS spectrum of the original HRP tryptic digests (10 ng μL^{-1}) without enrichment. Three peaks labeled in the picture, assigned to glycosylated peptides, were observed, while peaks of nonglycosylated peptides were highly intense, which suppress the signals of glycosylated peptides. After

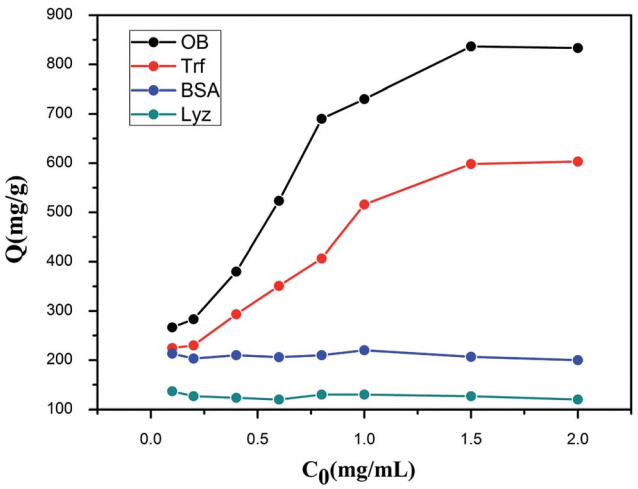

Fig. 5 Adsorption isotherm of glycoproteins (OVA, Trf) and non-glycoproteins (Lyz and BSA) on the Fe_3O_4/ZIF-8/APBA NPs.

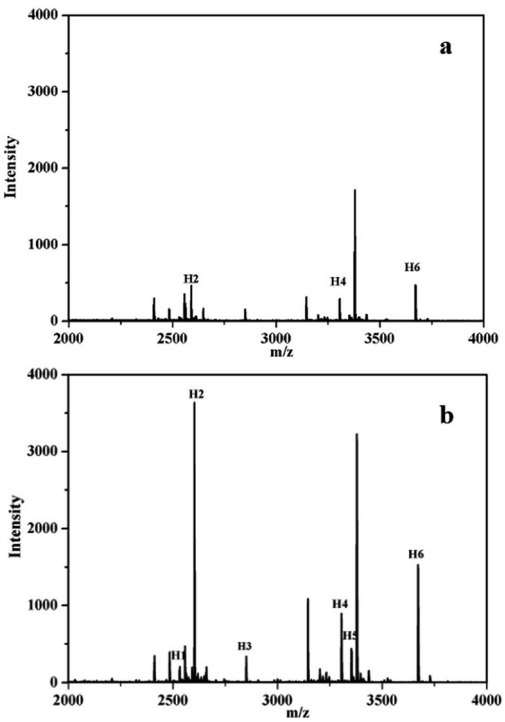

Fig. 7 MALDI-TOF mass spectra of HRP digests (10 ng μL^{-1}) obtained by direct analysis (a) and enrichment by Fe_3O_4/ZIF-8/APBA NPs (b).

enrichment by Fe_3O_4/ZIF-8/APBA NPs, six peaks of glycosylated peptides were identified (Fig. 7b). The detailed sequence of the identified 6 glycopeptides is listed in Table S1 ESI.† The enhanced enrichment capacity of each glycosylated peptide is dependent on the boronate affinity and on the synergistic interaction between glycopeptides and boric acid affinity of the synthetic Fe_3O_4/ZIF-8/APBA NPs.

Conclusions

In this study, a new strategy was proposed for the preparation of aminophenylboronic acid functionalized magnetic Fe_3O_4/ZIF-8 nanocomposite material. The assembly of Fe_3O_4 and ZIF-8 was achieved through electrostatic interaction and π–π stacking interaction. The nanocomposite substrate provided a high surface area to modify more boronic acid monomers and magnetic field to conveniently separate glycoproteins and glycopeptides. Due to the combination of surface modification of the composite substrates of Fe_3O_4 and ZIF-8 with boronate affinity, the synthesized Fe_3O_4/ZIF-8/APBA exhibited a high adsorption capacity and specific recognition toward the glycoproteins. Furthermore, Fe_3O_4/ZIF-8/APBA was successfully demonstrated by selective enrichment of low-abundance glycopeptides from HRP tryptic digests. The strategy for the fabrication of Fe_3O_4/ZIF-8/APBA provides a simple and effective approach, in which the boronic acid ligand was easily and efficiently functionalized on composite substrate materials. The Fe_3O_4/ZIF-8/APBA is expected to be a good receptor in the selective separation and enrichment of glycoproteins and glycopeptides in glycoproteomics.

Conflicts of interest

There are no conflicts to declare.

Acknowledgements

We greatly acknowledge financial support from the National Natural Science Foundation of China (21703102) and the Natural Science Foundation of Jiangsu Province, China (BK20170976).

Notes and references

1 D. Kolarich, P. H. Jensen, F. Altmann and N. H. Packer, *Nat. Protoc.*, 2012, **7**, 1285–1298.
2 Y. Tian and H. Zhang, *Proteomics: Clin. Appl.*, 2010, **4**, 124–132.
3 G. W. Hart and R. J. Copeland, *Cell*, 2010, **143**, 672–676.
4 G. Seeta Rama Raju, L. Benton, E. Pavitra and J. S. Yu, *Chem. Commun.*, 2015, **51**, 13248–13259.
5 D. F. Zielinska, F. Gnad, J. R. Wisniewski and M. Mann, *Cell*, 2010, **141**, 897–907.
6 C. Bi, Y. Zhao, L. Shen, K. Zhang, X. He, L. Chen and Y. Zhang, *ACS Appl. Mater. Interfaces*, 2015, **7**, 24670–24678.
7 L. Li, Y. Lu, Z. Bie, H.-Y. Chen and Z. Liu, *Angew. Chem., Int. Ed.*, 2013, **52**, 7451–7454.
8 Z. Xiong, H. Qin, H. Wan, G. Huang, Z. Zhang, J. Dong, L. Zhang, W. Zhang and H. Zou, *Chem. Commun.*, 2013, **49**, 9284–9286.
9 Y. Zhang, M. Kuang, L. Zhang, P. Yang and H. Lu, *Anal. Chem.*, 2013, **85**, 5535–5541.
10 H. Li and Z. Liu, *TrAC, Trends Anal. Chem.*, 2012, **37**, 148–161.
11 J. Chen, P. Shah and H. Zhang, *Anal. Chem.*, 2013, **85**, 10670–10674.
12 W. Zhang, X.-W. He, Y.-Q. Yang, W.-Y. Li and Y.-K. Zhang, *J. Mater. Chem. B*, 2013, **1**, 347–352.
13 A. Foettinger, A. Leitner and W. Lindner, *J. Chromatogr. A*, 2005, **1079**, 187–196.
14 Y. Zhang, W. Ma, D. Li, M. Yu, J. Guo and C. Wang, *Small*, 2014, **10**, 1379–1386.
15 W. Zhang, W. Liu, P. Li, H. Xiao, H. Wang and B. Tang, *Angew. Chem., Int. Ed.*, 2014, **53**, 12489–12493.
16 B. Jiang, Y. Liang, Q. Wu, H. Jiang, K. Yang, L. Zhang, Z. Liang, X. Peng and Y. Zhang, *Nanoscale*, 2014, **6**, 5616–5619.
17 X. Li, J. Feng, H. Zhu, C. Qu, J. Bai and X. Zheng, *RSC Adv.*, 2014, **4**, 33619–33625.
18 G. Wu, Y. Cheng, Z. Yang, Z. Jia, H. Wu, L. Yang, H. Li, P. Guo and H. Lv, *Chem. Eng. J.*, 2018, **333**, 519–528.
19 L. Liu, M. Yu, Y. Zhang, C. Wang and H. Lu, *ACS Appl. Mater. Interfaces*, 2014, **6**, 7823–7832.
20 H. Wang, Z. Bie, C. Lu and Z. Liu, *Chem. Sci.*, 2013, **4**, 4298–4303.
21 J. Lu, C. Deng, X. Zhang and P. Yang, *ACS Appl. Mater. Interfaces*, 2013, **5**, 7330–7334.
22 X. Zhang, J. Wang, X. He, L. Chen and Y. Zhang, *ACS Appl. Mater. Interfaces*, 2015, **7**, 24576–24584.
23 L. Jiang, M. E. Messing and L. Ye, *ACS Appl. Mater. Interfaces*, 2017, **9**, 8985–8995.
24 X. Zhang, X. He, L. Chen and Y. Zhang, *J. Mater. Chem.*, 2012, **22**, 16520–16526.
25 R. Ma, J. Hu, Z. Cai and H. Ju, *Nanoscale*, 2014, **6**, 3150–3156.
26 S. M. Cohen, *Chem. Sci.*, 2010, **1**, 32–36.
27 G. Ferey, *Chem. Soc. Rev.*, 2008, **37**, 191–214.
28 Z.-Y. Gu, Y.-J. Chen, J.-Q. Jiang and X.-P. Yan, *Chem. Commun.*, 2011, **47**, 4787–4789.
29 Y.-W. Zhang, Z. Li, Q. Zhao, Y.-L. Zhou, H.-W. Liu and X.-X. Zhang, *Chem. Commun.*, 2014, **50**, 11504–11506.
30 H. Bux, F. Liang, Y. Li, J. Cravillon, M. Wiebcke and J. Caro, *J. Am. Chem. Soc.*, 2009, **131**, 16000–16001.
31 H. Wang, L. Sun, Y. Li, X. Fei, M. Sun, C. Zhang, Y. Li and Q. Yang, *Langmuir*, 2011, **27**, 11609–11615.
32 X.-L. Zhao, D.-Y. Li, X.-W. He, W.-Y. Li and Y.-K. Zhang, *J. Mater. Chem. B*, 2014, **2**, 7575–7582.
33 H. Lan, N. Gan, D. Pan, F. Hu, T. Li, N. Long, H. Shen and Y. Feng, *J. Chromatogr. A*, 2014, **1365**, 35–44.
34 Z. Li, X. Li, Y. Zong, G. Tan, Y. Sun, Y. Lan, M. He, Z. Ren and X. Zheng, *Carbon*, 2017, **115**, 493–502.
35 Y. Zong, H. Xin, J. Zhang, X. Li, J. Feng, X. Deng, Y. Sun and X. Zheng, *J. Magn. Magn. Mater.*, 2017, **423**, 321–326.
36 X. Zhang, J. Feng, Y. Zong, H. Miao, X. Hu, J. Bai and X. Li, *J. Mater. Chem. C*, 2015, **3**, 4452–4463.

